EUROPHYSICS LETTERS 1 February 2004

Europhys. Lett., **65** (3), pp. 297–303 (2004)
DOI: 10.1209/epl/i2003-10100-9

Coherent electron wavepacket propagation and entanglement in array of coupled quantum dots

G. M. Nikolopoulos(*), D. Petrosyan and P. Lambropoulos(**)

Institute of Electronic Structure & Laser, FORTH
P.O. Box 1527, Heraklion 71110, Crete, Greece

(received 6 October 2003; accepted 26 November 2003)

PACS. 03.67.-a – Quantum information.
PACS. 73.63.Kv – Quantum dots.
PACS. 73.23.Hk – Coulomb blockade; single-electron tunneling.

Abstract. – We study the dynamics of single-electron transport in a linear array of tunnel-coupled quantum dots. We show that this system can serve as an ideal quantum channel, enabling a controlled transport and entanglement of electrons in a large-scale integrated quantum computer.

Introduction. – Arrays of coupled quantum dots (QDs), interacting with each other via electron tunneling and electrostatic interaction, offer an unprecedented possibility to construct at will and explore situations ranging from "artificial atoms and molecules" to fully solid-state many-body systems [1–4]. Given the controllable quantum properties of the electrons in such structures, the possibility of their application to schemes of quantum computers (QCs) [5] has not escaped attention [6, 7] largely motivated by their potentially unlimited scalability. The qubits of the QD-array–based QC would be represented by the spin states of single electrons confined in individual QDs [8, 9], with the two-qubit near-neighbor entanglement mediated by the controlled spin-exchange interaction. Thus, the building blocks of a scalable QC involve pairs of electrons and the possibility to interconnect distant parts of the quantum register via mobile qubits (electrons), under the crucial condition that coherence is preserved [5]. Motivated in part by the connection with QCs and in part by the need to understand the dynamics of electron wavepackets in the presence of disorder and fluctuations, with currently realistic parameters, we consider here a single-electron tunneling in a chain of QDs and establish the condition under which non-dispersive propagation of the wavepacket can be achieved. We then show how the combination of the single-electron coherent dynamics and controlled spin-exchange interaction between pairs of electrons in arrays of QDs could be envisioned in a large-scale integrated quantum register.

(*) Present address: Institut für Angewandte Physik - Hochschulstrasse 4a, 64289 Darmstadt, Germany.
(**) Also at the Department of Physics, University of Crete - Heraklion, Greece.

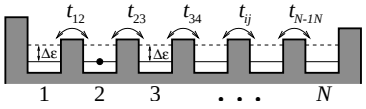

Fig. 1

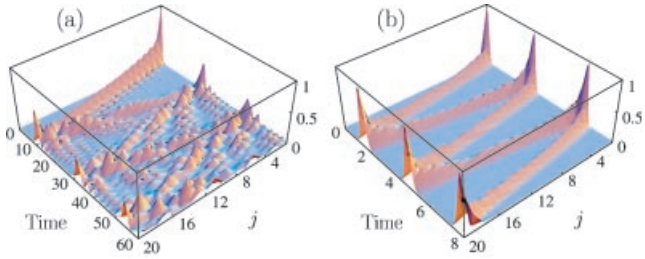

Fig. 2

Fig. 1 – Schematic drawing of the chain of tunnel-coupled QDs.

Fig. 2 – Single-electron transport in a chain of $N = 20$ QDs for the case of (a) equal couplings $t_{jj+1} = t_0$ $(1 \le j < N)$, and (b) optimal couplings $t_{jj+1} = t_0\sqrt{(N-j)j}$ between the dots. All parameters are normalized by t_0 and the time is in units of t_0^{-1}.

One excess electron in the chain. – We consider a linear array of N nearly identical QDs electrostatically defined in a two-dimensional electron gas by means of metallic gates on top of a semiconductor heterostructure [1, 2]. The evolution of the system is described by the extended Mott-Hubbard Hamiltonian [3]:

$$H = \sum_{j,\alpha} \varepsilon_{j\alpha} a^\dagger_{j\alpha} a_{j\alpha} + \frac{1}{2}\sum_j U n_j(n_j - 1) + \sum_{i<j,\alpha} t_{ij,\alpha}\left(a^\dagger_{i\alpha} a_{j\alpha} + \text{H.c.}\right) + \sum_{i<j} V_{ij} n_i n_j, \qquad (1)$$

where $a^\dagger_{j\alpha}$ $(a_{j\alpha})$ is the creation (annihilation) operator for an electron in state α with the single-particle energy $\varepsilon_{j\alpha}$, U is the on-site Coulomb repulsion, $n_j = \sum_\alpha a^\dagger_{j\alpha} a_{j\alpha}$ is the number operator of the j-th dot, $t_{ij,\alpha}$ are the coherent tunnel matrix elements which can be controlled by the external voltage applied to the gates defining the corresponding tunneling barriers between the adjacent dots $(j = i + 1)$, and V_{ij} describe the nearest-neighbor electrostatic interaction, $V_{ij} = V$. Interdot repulsion can be partially or fully screened $(V \approx 0)$ at will in the presence of a nearby conducting backgate. In the Coulomb blockade and tight-binding regime, when the on-site Coulomb repulsion and single-particle level-spacing $\Delta\varepsilon$ are much larger than the tunneling rates, $U > \Delta\varepsilon \gg t_{ij,\alpha}$ [10], only the equivalent states of neighboring dots are tunnel-coupled to each other. We, therefore, consider only a single doubly (spin-) degenerate level per dot $(\alpha \in \{\uparrow, \downarrow\})$, assuming further that the tunneling rates are spin independent $(t_{ij,\alpha} = t_{ij})$.

We study situations where one or more preselected QDs are initially doped with single electrons (see fig. 1). The preparation of such initial conditions can be accomplished by first applying a large negative voltage to the gates defining the electron confining potentials, while keeping the tunneling barriers low, thereby depleting the chain, and then doping one or more preselected QDs with single electrons by lowering the confining potentials and carefully manipulating the tunneling barriers between the dots and the external electron reservoir [8,9]. Finally, the system is isolated from the reservoir by closing the tunnelings at the two ends of the chain. To start the evolution, one then tunes the interdot tunneling rates to the preselected values. This process should be a) fast enough on the time scale of t_{ij}^{-1}, so that no appreciable change in the initial state of the system occurs during the switching time τ_{sw}, and b) adiabatic, so that no non-resonant coupling between the dots is induced: $\Delta\varepsilon^{-1}, U^{-1} < \tau_{\text{sw}} < t_{ij}^{-1}$.

In this paper we consider a chain of QDs that contains one excess electron; the problem of two interacting electrons will be addressed elsewhere [11]. Since the Hamiltonian (1)

preserves the number and spin state of electrons, the total wave function reads $|\psi_1(\tau)\rangle = \sum_{j,\alpha}^{N} A_j^\alpha(\tau)\,|j_\alpha\rangle$, where $|j_\alpha\rangle \equiv a_{j\alpha}^\dagger\,|0_1,\cdots,0_N\rangle$ denotes the state with one electron having spin α at the j-th dot. The Schrödinger equation yields

$$i\frac{\mathrm{d}A_j^\alpha}{\mathrm{d}\tau} = \varepsilon_j A_j^\alpha + t_{j-1j}A_{j-1}^\alpha + t_{jj+1}A_{j+1}^\alpha, \tag{2}$$

where $t_{01} = t_{NN+1} = 0$ and $\hbar = 1$. Clearly, the two sets of these amplitude equations with $\alpha = \uparrow$ and $\alpha = \downarrow$ are equivalent and decoupled from each other. Therefore, an arbitrary initial spin state of the electron is preserved throughout the evolution, assuming that the spin decoherence is vanishingly small on the time scale of t_{ij}^{-1}. Experimental measurement of spin-relaxation times indicate sub-MHz rates [12].

In fig. 2(a) we plot the time evolution of occupation probabilities $\langle\psi_1|\,n_j\,|\psi_1\rangle$ of $N = 20$ QDs along a uniform ($\varepsilon_j = \varepsilon_0$, $t_{ij} = t_0$) chain, isolated from the environment, for the initial state $|\psi_1(0)\rangle = |1_\alpha\rangle$. The initially localized electron wavepacket propagates along the chain and spreads to a number of dots. When the leading edge of the wavepacket is reflected from the end of the chain, its forward and backward propagating components begin to interfere with each other, which, after several reflections, results in a complete delocalization of the electron over the entire chain. This behavior can be readily understood from the analytic solution for the amplitudes

$$A_j^\alpha = \frac{2}{N+2}\sum_{k=1}^{N}\exp\left[-i2t_0\tau\cos\left(\frac{k\pi}{N+1}\right)\right]\sin\left(\frac{jk\pi}{N+1}\right)\sin\left(\frac{k\pi}{N+1}\right),$$

which shows that the eigenstates of the system oscillate with incommensurate frequencies $\lambda_k = 2t_0\cos[k\pi/(N+1)]$, and thus the system never revives fully to its initial state. One can, however, achieve a non-dispersive transfer of the single-electron wavepacket between the two ends of the chain (fig. 2(b)) by judiciously choosing the tunneling rates according to $t_{jj+1} = t_0\sqrt{(N-j)j}$, which we shall refer to as optimal coupling. Then the solution for the amplitudes has the simple binomial form

$$A_j^\alpha = \binom{N-1}{j-1}^{1/2}[-i\sin(t_0\tau)]^{(j-1)}\cos(t_0\tau)^{(N-j)},$$

while the eigenstates of the system have commensurate frequencies $\lambda_k = t_0(2k-N-1)$. Therefore, the electron wavepacket oscillates in a perfectly periodic way between the first and the last dots, whose occupation probabilities are given, respectively, by $|A_1^\alpha|^2 = \cos(t_0\tau)^{2(N-1)}$ and $|A_N^\alpha|^2 = \sin(t_0\tau)^{2(N-1)}$. The results shown in fig. 2 have been obtained through the numerical solution of eqs. (2).

Parenthetically, we note that eq. (2) and its solutions for some special cases of single-electron propagation in a chain of QDs are similar to those obtained for molecular excitations through a ladder of vibrational levels [13]. Models developed in that context more than twenty-five years ago found no application, simply because a vibrational structure is too complex to be amenable to simple models of, for example, equidistant levels or exact levels of a harmonic oscillator. On the other hand, in the present case, one can easily contemplate fabricating almost any desired level and tunneling rates arrangement. Thus, models that were of only academic interest then, now become of practical relevance.

To examine the influence of disorder due to the structure imperfections, gate voltage fluctuations, electron-phonon interactions, etc. [1], we have performed numerical integration

of eqs. (2) with random fluctuations of the intradot energy levels and interdot couplings, which would result in a decoherence of the electron wavepacket propagation. Specifically, we have modeled the energy levels ε_j and the interdot couplings t_{ij} as Gaussian random variables, with mean values ε_0, t_0 and variances $\delta\varepsilon, \delta t < t_0$, respectively. Our numerical simulations showed [11] that even in the presence of considerable disorder ($\delta\varepsilon = 0.1t_0$ and $\delta t = 0.05t_0$, which, for typical experimental parameters [10], correspond to $\delta\varepsilon \sim 5\,\mu$eV and $\delta t \sim 2.5\,\mu$eV) the coherent dynamics of the single-electron wavepacket propagation persist over many (up to twenty, for optimal-coupling case) oscillation periods! On the time scale $\tau \sim \delta\varepsilon^{-1}, \delta t^{-1}$, however, the system decoheres significantly due to the inhomogeneity introduced by the energy and coupling randomness.

Entanglement of two electrons. – Material particles like electrons represent a promising alternative to circumvent communication and detection loopholes that occur during the tests of Bell inequalities [14]. Despite an ever-growing number of theoretical proposals [15], the experimental demonstration of entanglement generation and detection in condensed-matter systems is still an open issue. One of the hardest steps towards such a realization is the necessity of controllable spatial separation of the two constituents of the entangled pair [15]. A similar problem hinders the realization of large-scale solid-state QCs. One of the main difficulties of the existing proposals for integrated QD-based QCs [6, 8, 9] is that the qubits (electron spins) interact with the nearest neighbors only, and there is no efficient way of transferring the information between distant qubits (one can SWAP the qubit state with its neighbor qubit, then the latter with the next neighbor, etc., which is inefficient since each SWAP action requires precise dynamical control of the parameters). Our intention in this section is to show that employing the optimal coupling one can circumvent these difficulties.

We adopt here an entanglement scheme (entangler) proposed in [6], which is based on the exchange interaction in a double-dot system where each QD is occupied by a single electron. When the interdot potential barrier is high, the tunneling is negligible, $t_e \simeq 0$, and the electronic orbitals are well localized at the corresponding dots. By lowering the interdot tunnel barrier, one can induce a finite overlap between the orbitals. Then the two electrons of this "artificial molecule" will be subject to a transient Heisenberg coupling [6, 15]:

$$H_s(\tau) = -J(\tau)\vec{S}_L \cdot \vec{S}_R, \tag{3}$$

where $\vec{S}_{L,R}$ are the spin-(1/2) operators for the left (L) and right (R) QDs, respectively, and $J(\tau) = 4t_e^2(\tau)/U$ is the effective time-dependent spin exchange constant. The effective Heisenberg Hamiltonian (3) can be obtained using eq. (1) after the adiabatic elimination of states $|j_\alpha, j_\beta\rangle$ corresponding to the double occupancy of dots $j = L, R$. If, initially, the two electrons have opposite spin states, $|\phi\rangle = |L_\uparrow, R_\downarrow\rangle$, and the pulsed Heisenberg coupling is applied for a specific duration such that $\theta \equiv \int J(\tau)\mathrm{d}\tau = \pi/2$, the square root of swap action ($\sqrt{\text{SWAP}}$) is realized. Then the resulting state of the system is the maximally entangled state $|\phi\rangle \to \frac{1}{\sqrt{2}}(\,|L_\uparrow, R_\downarrow\rangle + i\,|L_\downarrow, R_\uparrow\rangle)$.

Thus, a possible scheme, capable of producing mesoscopically separated EPR correlated pairs of electrons, relies on the the double-dot entangler that is embedded in a long chain of $N = 2M$ coupled QDs. To be specific, let us consider a symmetric structure depicted in fig. 3(a), in which the entangler, defined by the barriers B_L and B_R, is represented by the two middle dots of the chain, $L = M$ and $R = M + 1$. As discussed at the end of this section, the exact location of the entangler is not restrictive for the success of the scheme. The entanglement scenario then proceeds in three steps, illustrated in fig. 3(a)-(c), respectively. During the first step (fig. 3(a)), the potential barrier between the dots L and R is kept high and the exchange coupling is closed, $t_e = 0$. Therefore the two parts of the chain, composed of

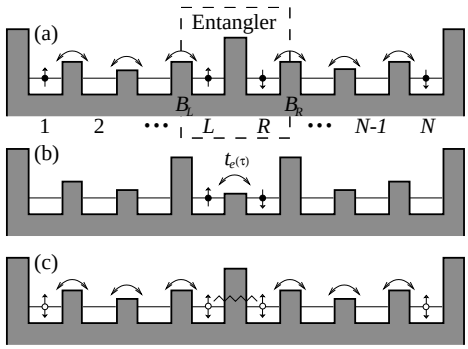

Fig. 3

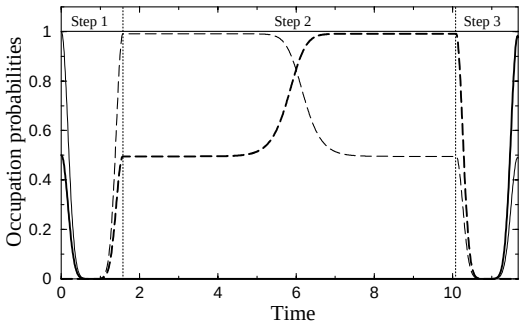

Fig. 4

Fig. 3 – Three-step generation of mesoscopically separated entangled electron pair. (a) In step 1, employing the optimal coupling for the chains 1–L and R–N, the two electrons are transferred to the entangler. Raising the barriers B_R and B_L, the entangler is temporarily isolated and the two electrons are trapped in dots L and R, respectively. (b) In step 2, a pulsed Heisenberg exchange coupling is applied, by turning on and off the tunneling matrix element $t_e(\tau)$. (c) In step 3, the two electrons are transferred back to dots 1 and N.

Fig. 4 – Numerical simulation of entangled-state generation in a chain of $N = 20$ QDs. The initial state is $|\psi_2(0)\rangle = |1_\uparrow, N_\downarrow\rangle$. The occupation probabilities of the two-electron states $|1_\uparrow, N_\downarrow\rangle$ (thin solid line), $|L_\uparrow, R_\downarrow\rangle$ (thin dashed line), $\frac{1}{\sqrt{2}}(|L_\uparrow, R_\downarrow\rangle + i\,|L_\downarrow, R_\uparrow\rangle)$ (thick dashed line), and $\frac{1}{\sqrt{2}}(|1_\uparrow, N_\downarrow\rangle + i\,|1_\downarrow, N_\uparrow\rangle)$ (thick solid line) are plotted as functions of time for the three-step process illustrated in fig. 3(a)-(c), respectively. The parameters are $\delta\varepsilon = 0.1t_0$, $\delta t = 0.05t_0$, $t_e^{\max} = 6t_0$, $U = 100t_0$ ($\Delta\tau \simeq 0.55t_0^{-1}$) and the optimal coupling is employed separately for each subchain 1–L and R–N.

dots 1–M and $(M+1)$–N, respectively, are decoupled from each other. The two unentangled electrons, initially located at dots 1 and N, are coherently transferred to the entangler by employing the optimal coupling in both parts of the chain. At time $\tau = \pi/(2t_0)$, when each electron reaches the corresponding dot of the entangler, the barriers B_L and B_R are pulsed to higher potentials so as to trap the corresponding electron. Note that, since $t_e = 0$, the trapping process need not occur simultaneously for both electrons. At the second step (fig. 3(b)), the exchange interaction is applied, by adiabatically turning on and off the tunneling matrix element t_e according to $t_e(\tau) = t_e^{\max}\mathrm{sech}[(\tau - \tau^{\max})/\Delta\tau]$, where $t_e^{\max}$ is the peak amplitude of the pulse and $\Delta\tau$ is its width. These parameters must be chosen such that the pulse area θ satisfies $\theta = \pi/2$, which yields $(t_e^{\max})^2\Delta\tau = \pi U/16$. At the same time, according to the adiabaticity criteria [6], the conditions $\Delta\tau^{-1}, t_e^{\max} \ll \Delta\varepsilon, U$ should be satisfied. Finally, at the third step (fig. 3(c)), the barriers B_L and B_R are reset to their initial values and the two electrons propagate along the chain and after time $\tau = \pi/(2t_0)$ become fully localized at the opposite ends of the chain, at dots 1 and N.

If the two electrons are prepared initially in the opposite spin states, $|\psi_2\rangle = |1_\uparrow, N_\downarrow\rangle$, during the three-step process the system will evolve into the maximally entangled state $|\psi_2\rangle \to \frac{1}{\sqrt{2}}(|1_\uparrow, N_\downarrow\rangle + i\,|1_\downarrow, N_\uparrow\rangle)$. If, on the other hand, the two electrons are prepared initially in the same spin state, $|1_\uparrow, N_\uparrow\rangle$ or $|1_\downarrow, N_\downarrow\rangle$, this state will remain unchanged (to within the phase factor $e^{i\theta/2}$). Finally, we note that if, during the second step, the exchange pulse area θ is equal to π (instead of $\pi/2$), the two electrons will swap their states $|1_\alpha, N_\beta\rangle \to i\,|1_\beta, N_\alpha\rangle$.

We have performed numerical simulations of the above scenario for an even total number of nearly identical QDs and the initial state $|\psi_2\rangle = |1_\uparrow, N_\downarrow\rangle$. The evolution of the occupation

probabilities $|\langle\phi_i|\psi_2(\tau)\rangle|^2$ for the two-electron states $|\phi_0\rangle = |1_\uparrow, N_\downarrow\rangle$, $|\phi_1\rangle = |L_\uparrow, R_\downarrow\rangle$, $|\phi_2\rangle = \frac{1}{\sqrt{2}}(|L_\uparrow, R_\downarrow\rangle + i\,|L_\downarrow, R_\uparrow\rangle)$, and $|\phi_3\rangle = \frac{1}{\sqrt{2}}(|1_\uparrow, N_\downarrow\rangle + i\,|1_\downarrow, N_\uparrow\rangle)$ during the three stages of the process is plotted in fig. 4. One can see that the fidelity of the entangled-state generation at the end of the process is very high, $|\langle\phi_3|\psi_2(\tau_{\rm end})\rangle|^2 \simeq 0.98$. Employing the spin-sensitive single-electron transistors [16], one could then use this EPR pair to perform a test of Bell inequalities with material particles (electrons). The controlled two-electron coherent dynamics studied above could be also envisioned in an integrated quantum register. Such a register would be composed of a large number of sub-registers, each containing two or more adjacent qubits represented by spins of single electrons in individual QDs. The sub-registers are embedded in a two-dimensional array of *empty QDs*. In combination with the mechanism of controlling the tunnel-coupling between the dots, this two-dimensional grid would realize a flexible quantum channel, capable of connecting any pair of qubits within the register. Thus, to transfer the information, one connects distant sub-registers by a chain of empty QDs and arranges the optimal tunnel-coupling between the dots to achieve a non-dispersive propagation of the qubit, followed by its controlled entanglement or SWAP with a target qubit. We note that this scheme is analogous to a proposal for an integrated ion-trap–based QC [17]. There, in order to circumvent the difficulties associated with building a large-scale ion trap quantum register, it was proposed to use many small sub-registers, each containing only a few ions, and connect these sub-registers to each other via controlled qubit (ion) transfer to the interaction region (entangler) represented by yet another ion trap.

Before closing this section, let us address the issue of location of the entangler. Since, as was noted above, the two electrons need not arrive at the entangler simultaneously, it is not necessary to position the entangler in the middle of the chain or synchronize the propagation of the two electrons during the first and the last steps. Actually, the entangler can be realized by any pair of dots in the chain, and in particular, even by the first two dots. Then only the second electron, initially located at dot N, should be brought into the entangler to interact with the first electron.

Conclusions. – To conclude, we have studied the microscopic dynamics of single-electron transport in a linear array of tunnel-coupled quantum dots. We have established the condition under which non-dispersive propagation of the electron wavepacket can be achieved, which, in combination with spin-exchange interaction between two electrons located at adjacent QDs, paves the way for the implementation of a large-scale integrated QD-array–based quantum computer.

Before closing, we note that electron wavepacket propagation in arrays of tunnel-coupled QDs bears many analogies with spin-wave propagation in Ising spin chains [18], electromagnetic-wave propagation in nonlinear periodic media [19], and matter-wave propagation in optical lattices [20]. With an unprecedented control over system parameters, arrays of QDs can bridge several fields [21] by providing realistic systems for quantitative studies of the interplay between coherence, localization and fluctuations in a context which until now could only be thought of as academic.

REFERENCES

[1] KOUWENHOVEN L. P. *et al.*, *Mesoscopic Electron Transport*, Vol. **345**, edited by SOHN L., KOUWENHOVEN L. P. and SCHÖN G. (Kluwer, Dordrecht) 1997, pp. 105-214; REIMANN S. M. and MANNINEN M., *Rev. Mod. Phys.*, **74** (2002) 1283; VAN DER WIEL W. G. *et al.*, **75** (2003) 1.

[2] KOUWENHOVEN L. P. *et al.*, *Phys. Rev. Lett.*, **65** (1990) 361; WAUGH F. R. *et al.*, **75** (1995) 705.

[3] Stafford C. A. and Das Sarma S., *Phys. Rev. Lett.*, **72** (1994) 3590; Kotlyar R., Stafford C. A. and Das Sarma S., *Phys. Rev. B*, **58** (1998) 3989; Stafford C. A., Kotlyar R. and Das Sarma S., **58** (1998) 7091.
[4] Gurvitz S. A. and Prager Y. S., *Phys. Rev. B*, **53** (1996) 15932; Wegewijs M. R. and Nazarov Y. V., **60** (1999) 14318.
[5] Nielsen M. A. and Chuang I. L., *Quantum Computation and Quantum Information* (Cambridge University Press, Cambridge) 2000.
[6] Loss D. and DiVincenzo D. P., *Phys. Rev. A*, **57** (1998) 120; Burkard G., Loss D. and DiVincenzo D. P., *Phys. Rev. B*, **59** (1999) 2070; Schliemann J., Loss D. and MacDonald A. H., *Phys. Rev. B*, **63** (2001) 085311.
[7] Zanardi P. and Rossi F., *Phys. Rev. Lett.*, **81** (1998) 4752.
[8] Friesen M. *et al.*, *Phys. Rev. B*, **67** (2003) 121301(R).
[9] Elzerman J. M. *et al.*, *Phys. Rev. B*, **67** (2003) 161308; Vandersypen L. *et al.*, *Quantum Computing and Quantum Bits in Mesoscopic Systems* (Kluwer Academic, Dordrecht) 2002.
[10] Typically, in $\sim$ 50 nm size GaAs/AlGaAs QDs, separated by $\sim$ 100 nm, $t_{ij} \sim 0.05$ meV, $\Delta\varepsilon \sim 0.4$ meV, $U \sim 10$ meV, and at dilution-refrigerator temperatures $T \sim$ 2–10 mK the thermal energy $k_{\mathrm{B}}T \sim 0.2$–$1\,\mu$eV [1].
[11] Nikolopoulos G. M., Petrosyan D. and Lambropoulos P., in preparation.
[12] Fujisawa T., Tokura Y. and Hirayama Y., *Phys. Rev. B*, **63** (2001) R081304.
[13] Bialynicka-Birula Z. *et al.*, *Phys. Rev. A*, **16** (1977) 2048; Cook R. J. and Shore B. W., **20** (1979) 539.
[14] Maitre X., Oliver W. D. and Yamamoto Y., *Physica E*, **6** (2000) 301.
[15] Saraga D. S. and Loss D., *Phys. Rev. Lett.*, **90** (2003) 166803; Hu X. and Das Sarma S., *Double quantum dot turnstile as an electron spin entangler*, arXiv: cond-mat/0307024; Zhang P., Xue Q.-K., Zhao X.-G. and Xie X., *Generation of spatially-separated spin entanglement in a triple quantum dot system*, arXiv: cond-mat/0307037.
[16] Schoelkopf R. J. *et al.*, *Science*, **280** (1998) 1238; Lu W. *et al.*, *Nature*, **423** (2003) 422.
[17] Kielpinski D., Monroe C. and Wineland D. J., *Nature*, **417** (2002) 709.
[18] Ernst R. R. *et al.*, *Principles of Nuclear Magnetic Resonance in One and Two Dimensions* (Claredon, Oxford) 1987.
[19] Kurizki G. *et al.*, *Progress in Optics*, edited by Wolf E., Vol. **42** (Elsevier, North-Holland) 2001, pp. 93-146.
[20] Jaksch D. *et al.*, *Phys. Rev. Lett.*, **81** (1998) 3108; Greiner M. *et al.*, *Nature*, **415** (2002) 39.
[21] Kramer B. and MacKinnon A., *Rep. Prog. Phys.*, **56** (1993) 1469.